

## Cluster decay of superheavy nuclei

D. N. Poenaru,<sup>1,2,\*</sup> R. A. Gherghescu,<sup>1,2</sup> and W. Greiner<sup>1</sup><sup>1</sup>Frankfurt Institute for Advanced Studies (FIAS), Ruth-Moufang-Str. 1, DE-60438 Frankfurt am Main, Germany<sup>2</sup>Horia Hulubei National Institute of Physics and Nuclear Engineering (IFIN-HH), P.O. Box MG-6, RO-077125 Bucharest-Magurele, Romania

(Received 21 February 2012; published 29 March 2012)

Calculations of half-lives of superheavy (SH) nuclei show an unexpected result: for some of them cluster radioactivity (CR) dominates over  $\alpha$  decay. We changed the concept of CR to allow emitted particles with  $Z_e > 28$  from parents with  $Z > 110$  (daughter around  $^{208}\text{Pb}$ ). We find a trend toward shorter half-lives and larger branching ratios relative to  $\alpha$  decay for heavier SHs. A table of measured masses along with theoretical tables are used to determine  $Q$  values.

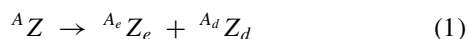
DOI: [10.1103/PhysRevC.85.034615](https://doi.org/10.1103/PhysRevC.85.034615)

PACS number(s): 23.70.+j, 23.60.+e, 21.10.Tg, 27.90.+b

### I. INTRODUCTION

Superheavy (SH) elements with atomic numbers  $Z = 104$ – $118$  have been synthesized with cold fusion reactions [1–3] or with hot fusion induced by  $^{48}\text{Ca}$  projectiles [4–6]. The majority of proton-rich SH nuclides are identified through the  $\alpha$  decay chains. Up to now only  $\alpha$  decay,  $\beta$  decay, and spontaneous fission of SH nuclei have been observed. Some papers on the theory of SHs [7–9], and stability calculations [10] are recently published.

We would like to discuss the competition of  $\alpha$  decay and cluster radioactivity (CR) [11,12], which may be important [13] in the region of the heaviest SHs. In this binary process, from one parent nucleus  $^AZ$ , one obtains an emitted particle  $^{A_e}Z_e$  and a daughter  $^{A_d}Z_d$ :



We have an indication of the possibility of extrapolating our calculations to this region from the results of the following calculations within the analytical supersymmetric fission (ASAF) model: the half-lives for  $^{128}\text{Sn}$  emission from  $^{256}\text{Fm}$  (the released energy  $Q = 252.129$  MeV) and for  $^{130}\text{Te}$  emission from  $^{262}\text{Rf}$  ( $Q = 274.926$  MeV) are given by  $\log_{10} T_{Fm}(s) = 4.88$  and  $\log_{10} T_{Rf}(s) = 0.53$ , respectively. They are in agreement with experimental values for spontaneous fission [14]: 4.02 and 0.32, respectively.

Since 1984 [15] the following CR has been experimentally confirmed [16,17] in heavy parent nuclei with  $Z = 87$  to 96:  $^{14}\text{C}$ ,  $^{20}\text{O}$ ,  $^{23}\text{F}$ ,  $^{22,24}$ – $^{26}\text{Ne}$ ,  $^{28,30}\text{Mg}$ , and  $^{32,34}\text{Si}$ . The employed techniques [18] are: semiconductor telescope; magnetic spectrometers (SOLENO, Enge split pole); and solid state nuclear track detectors. The measured half-lives are in good agreement with predicted values within the ASAF model (see the review [19] and references therein). The shortest measured half-life of  $T_c = 10^{11.01}$  s corresponds to  $^{14}\text{C}$  radioactivity of  $^{222}\text{Ra}$ , and the largest branching ratio relative to  $\alpha$  decay,  $b_\alpha = T_\alpha/T_c$ , of  $10^{-8.9}$  was observed for  $^{14}\text{C}$  radioactivity of  $^{223}\text{Ra}$ . Consequently CR in the region of heavy transfrancium nuclei is a rare phenomenon.

Very frequently the daughter nucleus was the doubly magic  $^{208}\text{Pb}_{126}$  or one of its neighbors. This is the reason why we changed the concept of CR, previously [20] associated with a maximum  $Z_e^{\max} = 28$ . In the regions of SHs with  $Z > 110$ , we consider not only the emitted particles with atomic numbers  $2 < Z_e < 29$ , but also heavier ones up to

$$Z_e^{\max} = Z - 82, \quad (2)$$

allowing us to get for  $Z > 110$  an atomic number of the most probable emitted cluster  $Z_e > 28$  and a doubly magic daughter around  $^{208}\text{Pb}$ .

Besides the already mentioned supersymmetric fission theory, there are many other theoretical approaches of CR, e.g., Refs. [21–25]. Spontaneous emission of a charged particle from an atomic nucleus is explained as a quantum mechanical tunneling of a preformed cluster at the nuclear surface through the potential barrier [26]. Microscopic calculations of cluster formation probability and of barrier penetrability have been performed [24,25] by using the R matrix description of the process. The half-life  $T_c$  is expressed as

$$T_c = \frac{\hbar \ln 2}{\Gamma_c}, \quad (3)$$

where  $\Gamma_c$  is the decay width and  $\hbar$  is the reduced Planck constant (or Dirac constant). A universal decay law for  $\alpha$  emission and CR was recently developed [25] based on this theory.

Present calculations are performed within the ASAF model, very useful for the high number of combinations of parent-emitted cluster in order to check the metastability of SH parent nuclides with measured or calculated masses against many possible decay modes.

### II. THE MODEL

A crucial quantity for accuracy of half-life calculation is the released energy

$$Q = [M - (M_e + M_d)]c^2 \quad (4)$$

obtained as a difference between the parent  $M$  and the two decay product masses,  $M_e$  and  $M_d$ , in units of energy;  $c$  is the light velocity.

\*poenaru@fias.uni-frankfurt.de

The decay constant  $\lambda = \ln 2/T_c$  may be expressed by a product of three model dependent quantities  $\nu$ ,  $S$ , and  $P_s$ , where  $\nu$  is the frequency of assaults on the barrier per second,  $S$  is the preformation probability, and  $P_s$  is penetrability of external barrier, mainly of Coulomb nature. According to our method [27] the preformation in a fission theory is given by the penetrability of the internal part of the barrier.

A very large number of combinations of parent-emitted cluster has to be considered in a systematic search for new decay modes. The numerical calculation of three-fold integrals involved in numerical models are too time consuming. The large amount of computations can be performed in a reasonable time by using an analytical relationship for the half-life. We developed our ASAF model to fulfill this requirement. We started with the Myers-Swiatecki liquid drop model [28] adjusted with a phenomenological correction.

The half-life of a parent nucleus  $AZ$  against the split into a cluster  $A_e Z_e$  and a daughter  $A_d Z_d$ ,

$$T = [(h \ln 2)/(2E_v)] \exp(K_{ov} + K_s), \quad (5)$$

is calculated by using the WKB quasiclassical approximation, according to which the action integral is expressed as

$$K = \frac{2}{\hbar} \int_{R_a}^{R_b} \sqrt{2B(R)E(R)} dR, \quad (6)$$

with  $B = \mu$ ,  $K = K_{ov} + K_s$ , and  $E(R)$  replaced by  $[E(R) - E_{\text{corr}}] - Q$ , where  $E_{\text{corr}}$  is a correction energy similar to the Strutinsky shell correction, also taking into account the fact that the Myers-Swiatecki's liquid drop model (LDM) [28] overestimates fission barrier heights, and the effective inertia in the overlapping region is different from the reduced mass  $\mu$ . The turning points of the WKB integral are:  $R_a = R_i + (R_t - R_i)[(E_v + E^*)/E_b^0]^{1/2}$  and  $R_b = R_t E_c \{1/2 + [1/4 + (Q + E_v + E^*)E_l/E_c^2]^{1/2}\}/(Q + E_v + E^*)$ , where  $E^*$  is the excitation energy concentrated in the separation degree of freedom,  $R_i = R_0 - R_e$  is the initial separation distance,  $R_t = R_e + R_d$  is the touching point separation distance,  $R_j = r_0 A_j^{1/3}$  ( $j = 0, e, d$ ;  $r_0 = 1.2249$  fm) are the radii of parent, emitted, and daughter nuclei, respectively, and  $E_b^0 = E_i - Q$  is the barrier height before correction. The interaction energy at the top of the barrier, in the presence of a nonnegligible angular momentum  $lh$  is given by

$$E_t = E_c + E_l = e^2 Z_e Z_d / R_t + \hbar^2 l(l+1)/(2\mu R_t^2). \quad (7)$$

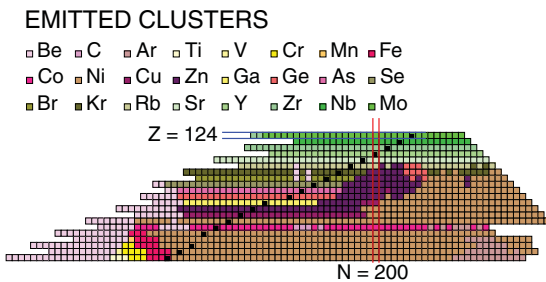


FIG. 1. (Color online) Chart of superheavy cluster emitters with atomic numbers  $Z = 104$  to  $124$ . The  $Q$  values are calculated using the FRDM95 mass tables. Black squares mark the Green approximation of the line of  $\beta$  stability.

The two terms of the action integral  $K$ , corresponding to the overlapping  $K_{ov}$  and separated  $K_s$  fragments, are calculated by analytical formulas (approximated for  $K_{ov}$  and exact for  $K_s$  in case of separated spherical shapes within the LDM):

$$K_{ov} = 0.2196(E_b^0 A_e A_d / A)^{1/2} (R_t - R_i) f(b), \quad (8)$$

$$f(b) = \sqrt{1 - b^2} - b^2 \ln \frac{1 + \sqrt{1 - b^2}}{b}, \quad (9)$$

$$K_s = 0.4392[(Q + E_v + E^*) A_e A_d / A]^{1/2} R_b J_{rc}, \quad (10)$$

$$J_{rc} = (c) \arccos \sqrt{g_c / (2 - c)} - [g_c (1 - r)]^{1/2} + \sqrt{1 - c} \ln F(c, r), \quad (11)$$

$$F(c, r) = \frac{2\sqrt{g_c(1-c)(1-r)} + 2 - 2c + cr}{r(2-c)}, \quad (12)$$

where  $g_c = 1 - c + r$ ,  $r = R_i / R_b$ ,  $c = r E_c / (Q + E_v + E^*)$ , and  $b^2 = (E_v + E^*) / E_b^0$ . In the absence of the centrifugal contribution ( $l = 0$ ), one has  $c = 1$ . We took  $E_v = E_{\text{corr}}$  in order to get a smaller number of parameters.

The potential barrier shape similar to that which we considered within the ASAF model was calculated by using the macroscopic-microscopic method [29], as a cut through the potential energy surface (PES) at a given mass asymmetry, usually the  $^{208}\text{Pb}$  valley or not far from it.

Half-life calculations are very sensitive to the released energy. Even with the updated table of experimental masses, atomic mass evaluation (AME) [30] many masses are still not available for new SHs. We have used not only this table for 3290 nuclides (2377 measured and 913 from the systematics) ending up at  $Z = 118$  but also some calculated masses, e.g., Liran-Marinov-Zeldes (LiMaZe01) [31,32], Koura-Tachibana-Ueno-Yamada (KTUY05) [33], and the finite-range droplet model (FRDM95) [34] with 1969 ( $Z = 82$  to  $126$ ,  $N \leq 184$ ), 9441 ( $Z = 2$  to  $130$ ,  $N \leq 200$ ), and 8979 ( $Z = 8$  to  $136$ ) masses, respectively.

One should observe the limitations present on every mass table. We are interested in SH parent nuclei with  $Z = 104$  to  $124$ . Those with  $Z = 119$  to  $124$  are not present on the AME mass table. The Green approximation of the line of  $\beta$  stability gives  $N_\beta = 166$  for  $Z = 104$ ,  $N_\beta = 186$  for  $Z = 114$ , and  $N_\beta = 206$  for  $Z = 124$ . In this way only neutron-deficient SHs are present on the AME mass table. Similarly, the majority of SHs from LiMaZe01 and KTUY05 are proton-rich nuclei. Only on the FRDM95 mass table we find both neutron-deficient and neutron-rich nuclei for all values of atomic numbers in the range  $104$ – $124$ .

In a systematic search for CR we calculate with the ASAF model for every parent nucleus  $AZ$  the half-lives of all combinations of pairs of fragments  $A_e Z_e$ ,  $A_d Z_d$  with  $2 < Z_d \leq Z_e^{\text{max}} = Z - 82$  conserving the hadron numbers  $Z_e + Z_d = Z$  and  $A_e + A_d = A$ .

### III. RESULTS

We would like to present the results obtained by using the AME experimental data as well as calculated masses LiMaZe01, KTUY05, and FRDM95. When using calculated

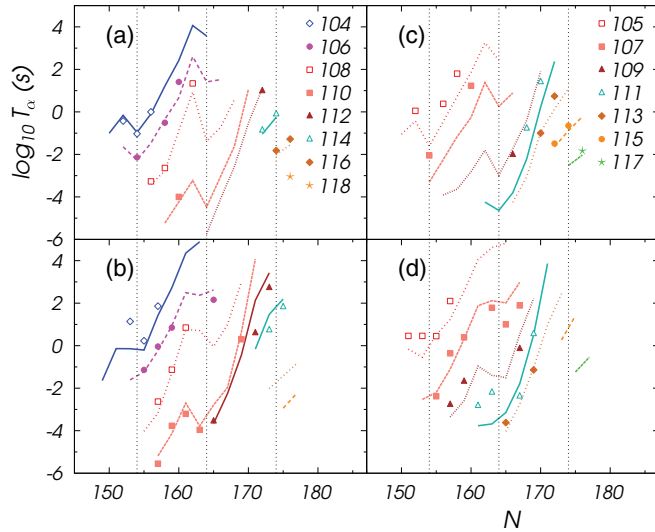


FIG. 2. (Color online) Decimal logarithm of the half-lives of SH nuclei against  $\alpha$  decay versus the neutron number of the parent nucleus in four groups of nuclides: (a) even-even, (b) even-odd, (c) odd-even, and (d) odd-odd. Calculations performed within the ASAF model. Experimental data marked with points. Vertical dashed lines correspond to  $N = 154, 164, 174$ .  $Q$  values are calculated using the AME mass tables.

masses for parent and daughter nuclei, we take into account the nuclides stable against one proton, two protons, one neutron, and two neutrons spontaneous emissions.

### A. Superheavy nuclei as cluster emitters

The chart of cluster emitters from Fig. 1 is obtained by associating to each parent only the most probable emitted

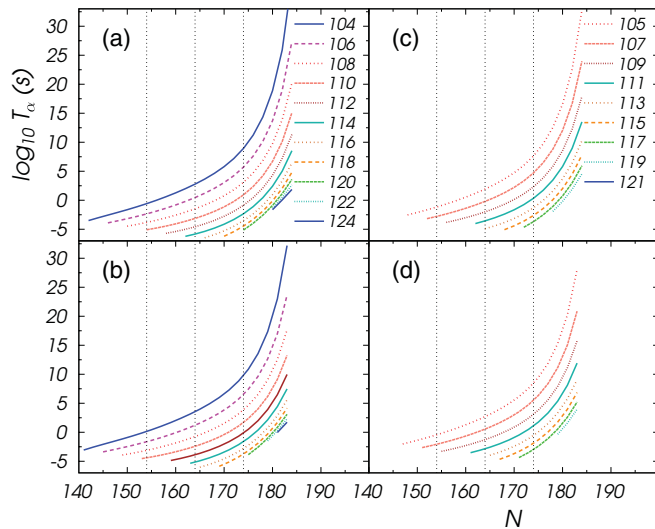


FIG. 3. (Color online) Decimal logarithm of the half-lives of SH nuclei against  $\alpha$  decay versus the neutron number of the parent nucleus in four groups of nuclides: (a) even-even, (b) even-odd, (c) odd-even, and (d) odd-odd. Calculations performed within the ASAF model. Vertical dashed lines correspond to  $N = 154, 164, 174$ .  $Q$  values are calculated using the LiMaZe01 mass tables.

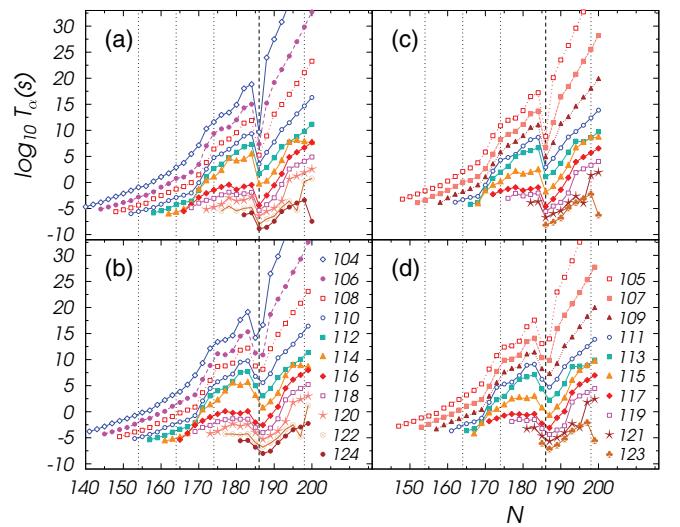


FIG. 4. (Color online) Decimal logarithm of the half-lives of the parent nucleus in four groups of nuclides: (a) even-even, (b) even-odd, (c) odd-even, and (d) odd-odd. Calculations performed within the ASAF model. Vertical dashed lines correspond to  $N = 154, 164, 174, 186, 198$ .  $Q$  values are calculated using the KTUY05 mass tables.

cluster in a systematic search based on FRDM95 masses. The black squares mark the Green approximation of the line of  $\beta$  stability.

As may be seen from the Fig. 1, besides emitted clusters with  $Z_e \leq 28$  (Be, C, Ar, Ti, V, Cr, Mn, Fe, Co, and Ni), many types of new CR with  $Z_e > 28$  are present on this chart: Cu, Zn, Ga, Ge, As, Se, Br, Kr, Rb, Sr, Y, Zr, Nb, and Mo. In other words the following atomic numbers of the most probable emitted heavy particle are obtained:  $Z_e = 4, 6, 18, 22, 23, 24, 25, 26, 27, 28, 29, 30, 31, 32, 33, 34, 35, 36, 37, 38, 39, 40, 41, 42$ . As we previously observed [20], many of the SH nuclides are  ${}^8\text{Be}$  emitters, but they have a very low branching ratio  $b_\alpha$ . *Most frequently occurs the doubly magic  ${}^{78}\text{Ni}$  radioactivity.*

In a few cases one has only one mass number for a given  $Z_e$ :  $A_e = 8$  for  $Z_e = 4$ ,  $A_e = 14$  for  $Z_e = 6$ ,  $A_e = 55$  for  $Z_e = 23$ , and  $A_e = 59$  for  $Z_e = 25$ . In other cases we also took only one color for every atomic number  $Z_e$ , despite the fact that one has various isotopes:  $A_e = 50, 52, 53$  for  $Z_e = 18$ ;  $53, 54$  for  $22$ ;  $58-60$  for  $24$ ;  $62, 64, 66$  for  $26$ ;  $63, 65, 71, 73, 75$  for  $27$ ;  $66, 68, 70-78$  for  $28$ ;  $73-80$  for  $29$ ;  $74, 76-82$  for  $30$ ;  $75, 77-83$  for  $31$ ;  $78, 80, 82-84, 86-88$  for  $32$ ;  $79-81, 83-89$  for  $33$ ;  $82$ ,

TABLE I. Comparison of standard rms deviations from experiment of half-life calculations performed within the ASAF model using different mass tables

Parent nuclei	$n$	$\sigma_{\text{AME}}$	$\sigma_{\text{LiMaZe01}}$	$\sigma_{\text{KTUY05}}$	$\sigma_{\text{FRDM95}}$
e-e	16	0.582	1.666	1.264	1.372
e-o	20	0.741	1.627	1.092	1.559
o-e	13	1.072	2.043	1.637	1.421
o-o	19	0.831	1.092	1.254	1.135

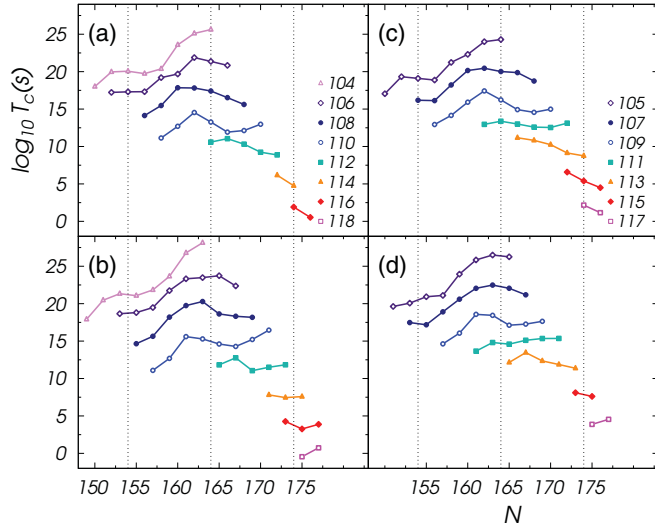


FIG. 5. (Color online) Decimal logarithm of the half-lives of SH nuclei against cluster decay versus the neutron number of the parent nucleus in four groups of nuclides: (a) even-even, (b) even-odd, (c) odd-even, and (d) odd-odd. Calculations performed within the ASAF model. Vertical dashed lines correspond to  $N = 154, 164, 174$ .  $Q$  values are calculated using the AME mass tables.

84–90 for 34; 85–93 for 35; 86–92, 94, 96, 98, 100 for 36; 89–102 for 37; 88–90, 92–96, 98, 100, 102, 104, 105 for 38; 96–108 for 39; 95–110 for 40; 103–113 for 41, and 100, 102, 104, 106–110, 112–115 for  $Z_e = 42$ .

**B.  $\alpha$  decay half-lives**

In Fig. 2 we compare the calculated half-lives of SHs against  $\alpha$  decay based on AME mass tables within the ASAF model with experimental data in four groups of parent nuclei:

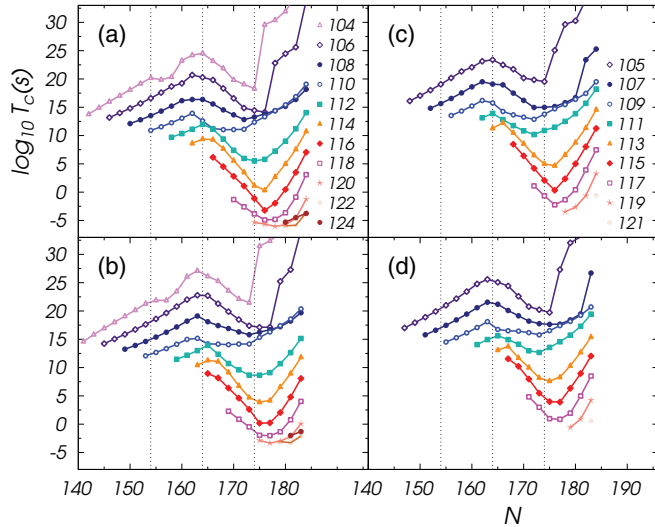


FIG. 6. (Color online) Decimal logarithm of the half-lives of SH nuclei against cluster decay versus the neutron number of the parent nucleus in four groups of nuclides: (a) even-even, (b) even-odd, (c) odd-even, and (d) odd-odd. Calculations performed within the ASAF model. Vertical dashed lines correspond to  $N = 154, 164, 174$ .  $Q$  values are calculated using the LiMaZe01 mass tables.

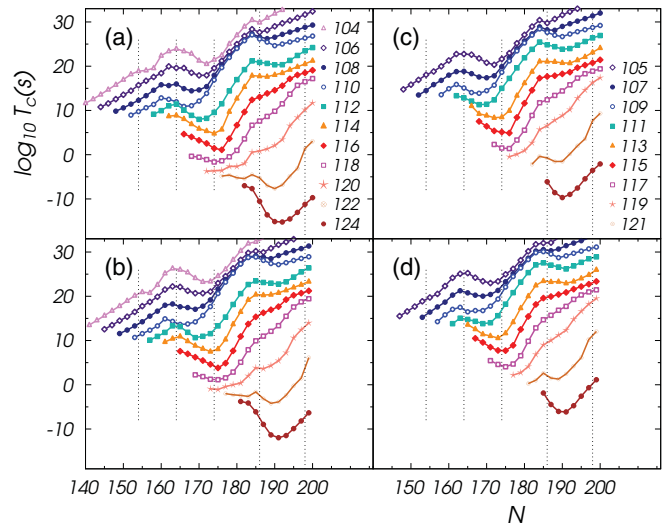


FIG. 7. (Color online) Decimal logarithm of the half-lives of SH nuclei against cluster decay versus the neutron number of the parent nucleus in four groups of nuclides: (a) even-even, (b) even-odd, (c) odd-even, and (d) odd-odd. Calculations performed within the ASAF model. Vertical dashed lines correspond to  $N = 154, 164, 174$ .  $Q$  values are calculated using the KTUY05 mass tables.

even-even (e-e), even-odd (e-o), odd-even (o-e), and odd-odd (o-o). The same quantity in Fig. 3 based on the LiMaZe01 mass table and Fig. 4 based on the KTUY05 mass table looks differently not showing the typical variations around the semimagic neutron numbers of the daughter  $N_d = 152, 162$ . Nevertheless, the overall accuracy is not very much affected as may be seen in the Table I, where we also included the results based on the FRDM95 mass table. On the other hand

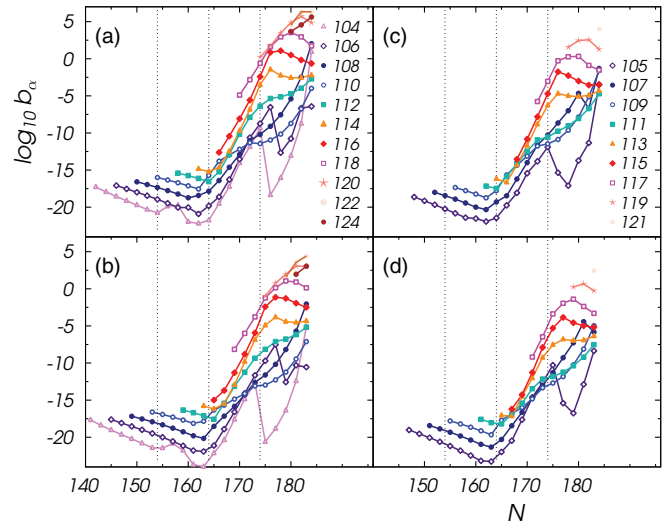


FIG. 8. (Color online) Decimal logarithm of the branching ratio relative to  $\alpha$  decay for cluster emission from superheavy nuclei versus the neutron number of the parent nucleus in four groups of nuclides: (a) even-even, (b) even-odd, (c) odd-even, and (d) odd-odd. Vertical dashed lines correspond to  $N = 154, 164, 174$ .  $Q$  values are calculated using the LiMaZe01 mass tables.



the minimum around  $N = 186$  is due to the assumed magicity of the daughter neutron number  $N_d = 184$ .

An estimation of the accuracy gives the standard rms deviation of  $\log_{10} T$  values:

$$\sigma = \left\{ \sum_{i=1}^n [\log_{10}(T_i/T_{\text{exp}})]^2 / (n-1) \right\}^{1/2}. \quad (13)$$

As may be seen in Table I the best reproduction of experimental values is obtained by using AME masses to calculate  $Q$  values, as expected. It is followed by KTUY05 for e-e and e-o nuclei, by FRDM95 for o-e nuclei, and by LiMaZe01 for o-o SH parent nuclei. Lower values of  $\sigma$  for  $\alpha$  decay half-lives may be obtained [35] within our UNIV (universal curve) and semFIS (semiempirical) models.

The general trend toward a shorter half-life against  $\alpha$  decay for higher  $Z$  values is clearly seen in Figs. 2–4.

### C. Cluster decay half-lives

We present in Figs. 5–7, the half-lives of SH nuclei against CR in four groups of parent nuclei, based on  $Q$  values calculated with mass tables AME, LiMaZe01, and KTUY05, respectively. They are again shorter and shorter when the atomic number increases.

For a given  $N$  and  $Z$  number of the SH parent nucleus, the half-life against CR,  $T_c$ , in Fig. 5 is longer than the corresponding half-life against  $\alpha$  decay,  $T_\alpha$ , in Fig. 2. When the calculated mass tables with more SHs are used, as in Figs. 6 and 7, we can find several cases with  $T_c < T_\alpha$  for the heaviest parent nuclei.

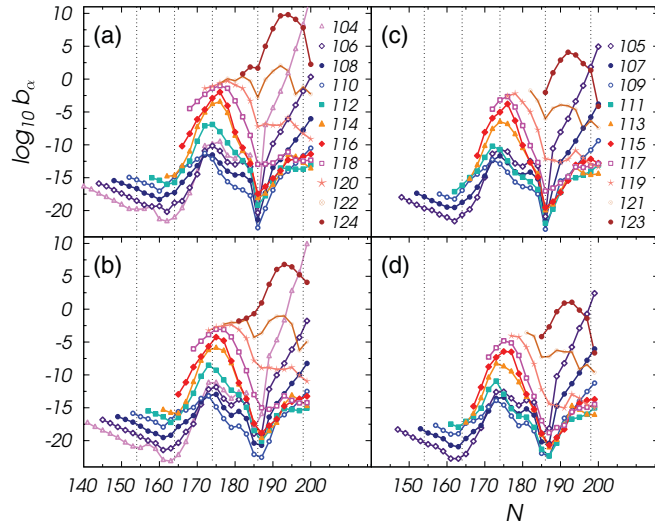


FIG. 9. (Color online) Decimal logarithm of the branching ratio relative to  $\alpha$  decay for cluster emission from superheavy nuclei versus the neutron number of the parent nucleus in four groups of nuclides: (a) even-even (b) even-odd (c) odd-even, and (d) odd-odd. Vertical dashed lines correspond to  $N = 154, 164, 174, 186, 198$ .  $Q$  values are calculated using the KTUY05 mass tables.

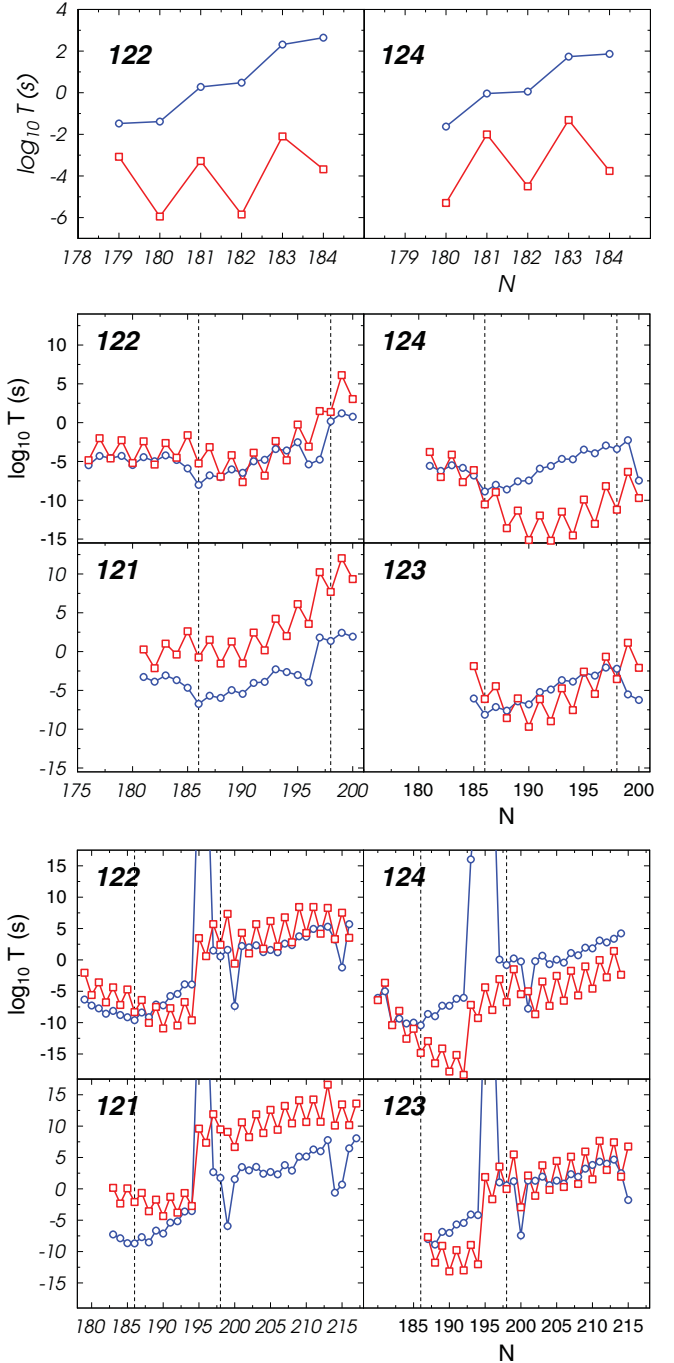


FIG. 10. (Color online) Decimal logarithm of the half-lives of superheavy nuclei with atomic numbers 121–124 against  $\alpha$  decay (blue circles) and CR (red squares) versus the neutron number of the parent nucleus.  $Q$  values are calculated using the (top) LiMaZe01, (middle) KTUY05, and (bottom) FRDM95 mass tables.

### D. Branching ratio relative to $\alpha$ decay

The general trend of a shorter half-life and a larger branching ratio when the atomic and mass numbers of the parent nucleus increases may be seen on the Figs. 8 and 9, obtained within the ASAF model by using the LiMaZe01 and KTUY05 mass tables, respectively, to calculate the  $Q$  values in four groups of parent nuclei: even-even, even-odd, odd-even,

and odd-odd. As in previous subsections, this kind of plots in four groups allow us to get smoother curves compared to what would be obtained if the even-odd staggering would be present. As to absolute values of  $T_c$  and  $b_\alpha$ , there is no guarantee of reliability until some measurements will be available. More elaborate models should be used (see, e.g., [36]) in order to estimate the competition of spontaneous fission.

If the calculated masses are reliable, then half-lives  $T_c$  shorter than 1 ns for SH nuclei with  $Z \geq 122$  and large neutron numbers (see Fig. 10) would make difficult or even impossible any identification measurement. It would be possible to find some interesting cases with  $T_c < T_\alpha$ ,  $b_\alpha > 1$  which could be measured (see Fig. 9). For example if  $Z = 122$ , the neutron number of the Green approximation of the line of  $\beta$  stability is  $N_\beta = 202$ , meaning that some neutron-deficient isotopes of 122 with  $N > 188$  could have  $b_\alpha > 1$ . An increase in  $Q$  value of  $\Delta Q = 1.08$  MeV (from 273.49 to 274.57) produces a shorter half-life by 1.2 orders of magnitude,  $\log_{10} T_c(s)$  from 6.58 to 5.38 for  $^{81}\text{As}$  emission from  $^{287}\text{115}$ . Similarly for  $\Delta Q = 0.87$  MeV one has a one order of magnitude shorter half-life for  $^{85}\text{Se}$  radioactivity of  $^{293}\text{116}$ .

The pronounced minimum of the branching ratio at  $N = 186$  in Fig. 9 is the result of the strong shell effect of the assumed magic number of neutrons of the daughter  $N_d = 184$  present in the KTUY05 masses. The half-life of  $\alpha$  decay of a SH nucleus with  $N = 186$  neutron number leading to a more stable daughter with magic neutron number  $N_d = 184$  is shorter by some orders of magnitude compared to the  $\alpha$  decay of a SH with  $N = 184$ . Similar results were obtained using the FRDM95 masses (see Fig. 10).

In Fig. 10 we can compare the absolute values of half-lives for  $\alpha$  decay and CR for SHs with  $Z = 121$  to 124 calculated within the ASAF model using different mass tables. The even-odd staggering is more pronounced for CR than for  $\alpha$  decay, leading to larger  $b_\alpha$  for even  $N$  nuclides compared to the neighboring odd  $N$  ones. This effect produces an alternation of  $b_\alpha$  values for successive even and odd neutron numbers.

Half-lives  $T_c < T_\alpha$  are found for neutron-deficient SHs present on LiMaZe01 mass tables (at the top of Fig. 10). A transition from  $b_\alpha < 1$  for  $Z = 121$  to  $b_\alpha > 1$  when  $Z$  increases toward  $Z = 124$  may be clearly seen in the central and bottom panels. A sharp decrease of  $Q_\alpha$  values calculated with FRDM95 masses around  $N = 196$  produces very high  $T_\alpha$  at the bottom of Fig. 10.

We may better illustrate the importance of reliable mass values by selecting in Table II a few cases of SHs with  $Z > 120$  present on Fig. 10. As can be seen from this table, large differences in  $Q$  values for  $\alpha$  decay calculated with various mass tables occur very frequently and make an important contribution to the broad range of branching ratios  $b_\alpha$  shown in the last column. Even the most probable emitted cluster can differ as in the case of the  $^{304}\text{124}$  parent for which  $^{98}\text{Mo}$  results in calculations of released energy based on LiMaZe01,  $^{95}\text{Zr}$  based on KTUY05, and  $^{96}\text{Zr}$  based on FRDM95.

In conclusion, by changing the concept of CR to allow spontaneous emission of heavy particles with atomic numbers larger than 28 from SHs with  $Z > 110$  (daughter nuclei around the doubly magic  $^{208}\text{Pb}$ ), we found that calculated half-lives  $T_c$  against CR and the branching ratios relative to  $\alpha$  decay

TABLE II.  $Q$  values in MeV, half-lives, and branching ratios for the most probable CR of a few SH neutron-deficient nuclei, obtained by using three mass tables: LiMaZe01, KTUY05, and FRDM95.

Parent	Mass table	$Q_\alpha$	$\log_{10} T_\alpha(s)$	Emit.C	$Q_c$	$\log_{10} T_c(s)$	$\log_{10} b_\alpha$
$^{302}\text{122}$	LiMaZe01	11.206	-1.39	$^{96}\text{Zr}$	337.86	-5.95	4.56
	KTUY05	13.055	-5.46	$^{96}\text{Zr}$	337.21	-5.20	-0.25
	FRDM95	14.045	-7.27	$^{96}\text{Zr}$	337.55	-5.60	-1.67
$^{303}\text{122}$	LiMaZe01	10.839	0.28	$^{96}\text{Zr}$	337.66	-3.28	3.56
	KTUY05	12.885	-4.45	$^{96}\text{Zr}$	336.91	-2.41	-2.04
	FRDM95	14.705	-7.73	$^{96}\text{Zr}$	337.91	-3.58	-4.15
$^{304}\text{122}$	LiMaZe01	10.480	0.48	$^{96}\text{Zr}$	337.18	-5.85	6.33
	KTUY05	12.795	-4.98	$^{96}\text{Zr}$	336.79	-5.40	0.42
	FRDM95	14.815	-8.58	$^{96}\text{Zr}$	337.97	-6.76	-1.82
$^{304}\text{124}$	LiMaZe01	11.192	-0.04	$^{98}\text{Mo}$	352.86	-2.00	1.96
	KTUY05	13.735	-5.57	$^{95}\text{Zr}$	346.07	-3.78	-1.79
	FRDM95	13.435	-5.01	$^{96}\text{Zr}$	345.79	-3.65	-1.36
$^{305}\text{124}$	LiMaZe01	10.862	0.05	$^{100}\text{Mo}$	351.88	-4.50	4.55
	KTUY05	13.705	-6.22	$^{100}\text{Mo}$	354.08	-7.01	0.79
	FRDM95	16.325	-10.37	$^{100}\text{Mo}$	357.04	-10.40	0.03
$^{306}\text{124}$	LiMaZe01	10.521	1.73	$^{100}\text{Mo}$	351.34	-1.31	3.04
	KTUY05	13.675	-5.49	$^{100}\text{Mo}$	353.75	-4.13	-1.37
	FRDM95	16.055	-9.3	$^{100}\text{Mo}$	357.13	-8.12	-1.25
$^{307}\text{124}$	LiMaZe01	10.202	1.86	$^{102}\text{Mo}$	349.81	-3.76	5.62
	KTUY05	13.475	-5.83	$^{102}\text{Mo}$	353.19	-7.67	1.84
	FRDM95	16.135	-10.14	$^{102}\text{Mo}$	357.48	-12.57	2.43

are showing a trend toward shorter  $T_c$  and larger  $b_\alpha$  for the heaviest SHs. It is possible to find regions of SHs where the half-lives for CR are shorter than those against  $\alpha$  decay. The accuracy of calculated masses in the region of heaviest SHs should be improved in order to make reliable predictions of half-lives.

## ACKNOWLEDGMENTS

This work was partially supported by the Deutsche Forschungsgemeinschaft and partially within the IDEI Programme under Contracts No. 43/05.10.2011 and No. 42/05.10.2011 with UEFISCDI, Bucharest.

- 
- [1] S. Hofmann, G. Münzenberg, *Rev. Mod. Phys.* **72**, 733 (2000).  
 [2] S. Hofmann, *Radiochim. Acta* **99**, 405 (2011).  
 [3] K. Morita *et al.*, *J. Phys. Soc. Jpn.* **76**, 045001 (2007).  
 [4] Y. T. Oganessian, *J. Phys. G: Nucl. Part. Phys.* **34**, R165 (2007).  
 [5] Y. T. Oganessian *et al.*, *Phys. Rev. Lett.* **104**, 142502 (2010).  
 [6] Y. T. Oganessian, *Radiochim. Acta* **99**, 429 (2011).  
 [7] W. Greiner and D. N. Poenaru, in *Cluster Structure of Atomic Nuclei*, edited by M. Brenner (Research Signpost, Trivandrum, India, 2010), Chap. 5, pp. 119–146.  
 [8] A. Sobiczewski, *Radiochim. Acta* **99**, 395 (2011).  
 [9] V. I. Zagrebaev, A. V. Karpov, and W. Greiner, *Phys. Rev. C* **85**, 014608 (2012).  
 [10] P. Jachimowicz, M. Kowal, and J. Skalski, *Phys. Rev. C* **83**, 054302 (2011).  
 [11] A. Sandulescu, D. N. Poenaru, and W. Greiner, *Sov. J. Part. Nucl.* **11**, 528 (1980).  
 [12] Encyclopaedia Britannica Online, 2011 [<http://www.britannica.com/EBchecked/topic/465998/>].  
 [13] D. N. Poenaru, R. A. Gherghescu, and W. Greiner, *Phys. Rev. Lett.* **107**, 062503 (2011).  
 [14] D. C. Hoffman, T. M. Hamilton, and M. R. Lane, in *Nuclear Decay Modes*, edited by D. N. Poenaru (Institute of Physics Publishing, Bristol, 1996), Chap. 10, pp. 393–432.  
 [15] H. J. Rose and G. A. Jones, *Nature (London)* **307**, 245 (1984).  
 [16] R. Bonetti and A. Guglielmetti, *Rom. Rep. Phys.* **59**, 301 (2007).  
 [17] D. N. Poenaru, Y. Nagame, R. A. Gherghescu, and W. Greiner, *Phys. Rev. C* **65**, 054308 (2002); **66**, 049902(E) (2002).  
 [18] *Experimental Techniques in Nuclear Physics*, edited by D. N. Poenaru and W. Greiner (Walter de Gruyter, Berlin, 1997).  
 [19] D. N. Poenaru and W. Greiner, in *Clusters in Nuclei Vol. 1*, edited by C. Beck, Lecture Notes in Physics, Vol. 818 (Springer, Berlin, 2010), Chap. 1, pp. 1–56.  
 [20] D. N. Poenaru, D. Schnabel, W. Greiner, D. Mazilu, and R. Gherghescu, *At. Data Nucl. Data Tables* **48**, 231 (1991).  
 [21] M. Warda and L. M. Robledo, *Phys. Rev. C* **84**, 044608 (2011).  
 [22] R. Blendowske and H. Walliser, *Phys. Rev. Lett.* **61**, 1930 (1988).  
 [23] *Nuclear Decay Modes*, edited by D. N. Poenaru (Institute of Physics Publishing, Bristol, 1996).  
 [24] R. G. Lovas, R. J. Liotta, A. Insolia, K. Varga, and D. S. Delion, *Phys. Rep.* **294**, 265 (1998).  
 [25] C. Qi, F. R. Xu, R. J. Liotta, and R. Wyss, *Phys. Rev. Lett.* **103**, 072501 (2009).  
 [26] G. Gamow, *Z. Phys.* **51**, 204 (1928).  
 [27] D. N. Poenaru and W. Greiner, *Physica Scripta* **44**, 427 (1991).  
 [28] W. D. Myers and W. J. Swiatecki, *Nucl. Phys. A* **81**, 1 (1966).  
 [29] D. N. Poenaru, R. A. Gherghescu, and W. Greiner, *Phys. Rev. C* **73**, 014608 (2006).  
 [30] G. Audi, and W. Meng (private communication).  
 [31] S. Liran, A. Marinov, and N. Zeldes, *Phys. Rev. C* **62**, 047301 (2000); arXiv:nucl-th/0102055v1.  
 [32] S. Liran, A. Marinov, and N. Zeldes, *Phys. Rev. C* **66**, 024303 (2002).  
 [33] H. Koura, T. Tachibana, M. Uno, and M. Yamada, *Prog. Theor. Phys.* **113**, 305 (2005).  
 [34] P. Möller, J. R. Nix, W. D. Myers, and W. J. Swiatecki, *At. Data Nucl. Data Tables* **59**, 185 (1995).  
 [35] D. N. Poenaru, I. H. Plonski, and W. Greiner, *Phys. Rev. C* **74**, 014312 (2006).  
 [36] R. Smolanczuk, J. Skalski, and A. Sobiczewski, *Phys. Rev. C* **52**, 1871 (1995).